

- Mackenzie, D. R. Pring, M. J. Bassett, C. D. Chase, *Proc. Natl. Acad. Sci. U.S.A.* **85**, 2714 (1988).
19. D. A. Clayton, J. N. Doda, E. C. Friedberg, *Proc. Natl. Acad. Sci. U.S.A.* **71**, 2777 (1974); J.-I. Hayashi, Y. Tagashira, M. C. Yoshida, *Exp. Cell Res.* **160**, 387 (1985).
20. I. B. Dawid, I. Horak, H. G. Coon, *Genetics* **78**, 459 (1974); I. Horak, H. G. Coon, I. B. Dawid, *Proc. Natl. Acad. Sci. U.S.A.* **71**, 1828 (1974).
21. A. E. Tomkinson and S. Linn, *Nucleic Acids Res.* **14**, 9579 (1986); D. D. Chang and D. A. Clayton, *EMBO J.* **6**, 409 (1987); *Science* **235**, 1178 (1987); *Cell* **56**, 131 (1989).
22. P. J. Farabaugh, U. Schmeissner, M. Hofer, J. H. Miller, *J. Mol. Biol.* **126**, 847 (1978); C. W. Jones and F. C. Kafatos, *J. Mol. Evol.* **19**, 87 (1982); A. Efstratiadis *et al.*, *Cell* **21**, 653 (1980).
23. A. Larsen and H. Weintraub, *Cell* **29**, 609 (1982); E. A. Schon *et al.*, *ibid.* **35**, 837 (1983).
24. R. D. Wells *et al.*, *FASEB J.* **2**, 2939 (1988).
25. J. G. McCarthy and S. M. Heywood, *Nucleic Acids Res.* **12**, 6473 (1984).
26. V. I. Lyamichiev, S. M. Mirkin, M. D. Frank-Kamenetskii, *J. Biomol. Struct. Dyn.* **3**, 327 (1985); *ibid.*, p. 667; S. M. Mirkin *et al.*, *Nature* **330**, 495 (1987); O. N. Voloshin, S. M. Mirkin, V. I. Lyamichiev, B. P. Belotserkovskii, M. D. Frank-Kamenetskii, *ibid.* **333**, 475 (1988); H. Htun and J.

- E. Dahlberg, *Science* **241**, 1791 (1988); B. H. Johnston, *ibid.*, p. 1800.
27. We thank S. Shanske, G. M. Fabrizi, J. Sadlock, and A. Lombes for assistance with the experiments. This work was supported by Center Grant NS11766 from NIH and by a Center Grant from the Muscular Dystrophy Association. E.A.S. was supported by the Aaron Diamond Foundation, H.N. by a fellowship from Mr. and Mrs. Libero Danesi, and C.T.M. was supported by the Brazilian Research Council (CNPq); R.R. is a fellow of the Muscular Dystrophy Association.

29 November 1988; accepted 21 February 1989

Two Molecular Transitions Influence Cardiac Sodium Channel Gating

DAVID T. YUE,* JOHN H. LAWRENCE, EDUARDO MARBAN

Sodium channels from diverse excitable membranes are very similar in their structure, yet surprisingly heterogeneous in their behavior. The processes that govern the opening and closing of sodium channels have appeared difficult to describe in terms of a single, unifying molecular scheme. Now cardiac sodium channels have been analyzed by high-resolution single-channel recordings over a broad range of potentials. Channels exhibited both complex and simple gating patterns at different voltages. Such behavioral diversity can be explained by the balance between two molecular transitions whereby channels can exit the open state.

VOLTAGE-DRIVEN CONFORMATIONAL changes that control the opening and closing of Na⁺ channels form the molecular basis for membrane excitability. Despite the remarkable structural similarity of Na⁺ channels from diverse sources (1), their functional gating properties have proven quite heterogeneous. Although Na⁺ channels in some neuronal cells open briefly and only once with depolarization (2), the gating behavior in other neural preparations (3, 4) and heart (5–8) and skeletal muscle (9) is considerably more complex: channels open, close, and reopen many times before finally entering a long-lived inactivated state. We now report that single Na⁺ channels from heart cells can exhibit either simple or complicated patterns of gating, both of which can be explained by a single gating paradigm.

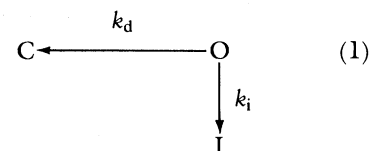
To overcome the difficulties presented by inevitable recording system noise and diminishing open channel flux at voltages positive to –20 mV, we increased the Na⁺ concentration in our pipettes ([Na⁺]_o) from the usual 140 to 425 mM and thereby raised open channel conductance from ~10 to 25 pS. This enabled the resolution of brief

unitary currents at voltages up to +20 mV (10, 11). We increased the osmolarity of the bath solution 1.5-fold to prevent patch rupture. Na⁺ channel gating was not appreciably changed by the increase in permeant ion concentration, as judged by comparison of individual sweeps, ensemble current averages, and open time histograms. We used cell-attached patches to avoid modifications of gating behavior known to develop with patch excision (12).

The improvement in resolution reveals two prominently distinct patterns of gating at different membrane potentials. During depolarizing pulses to –50 mV (Fig. 1A), representative sweeps demonstrate the complicated pattern of multiple reopenings described previously in heart cells (5–8). The time to first channel opening is rather dispersed, and the lifetime of single openings does not parallel the decay of ensemble average current (Fig. 1A, bottom row). In contrast, voltage steps to –20 mV, or greater, elicit simple gating behavior (Fig. 1, B and C). Channels appear to open almost immediately on depolarization and once per depolarizing pulse. Consequently, the duration of single openings generally tracks the time course of declining ensemble current.

Does such dichotomous gating behavior arise from two conformationally different gating modes (7, 9, 12, 13) favored at different voltages? The analysis below argues against this notion by demonstrating that the two gating patterns are explained when

the predictions of the standard gating model shown below (2, 3, 14) are considered in very different voltage ranges.



In this scheme there is a single open state (O), as required (15) by the predominantly single-exponential nature of open time histograms shown here and elsewhere (2, 3, 5–9, 12). In keeping with arguments presented elsewhere (2, 3, 6, 16), two principal pathways of exit from the open state are considered: one leading to a group of closed but available states (C) with rate constant k_d (deactivation) and the other to a group of absorbing, inactivated states (I) with rate constant k_i (inactivation).

Eyring rate theory enables us to predict the interaction of voltage with this model. This theory provides a simple link between the rate constants in Eq. 1 and the chemical and electrical components of the energy barriers encountered by channels leaving the open state (17). Thus,

$$k_d = k_d(0) \exp(+Q_d V)/(RT) \quad (2a)$$

$$k_i = k_i(0) \exp(+Q_i V)/(RT) \quad (2b)$$

where V is the transpatch voltage; $k_d(0)$ and $k_i(0)$ are the values of the respective rate constants at $V = 0$; Q_d and Q_i are the equivalent charge movements across the membrane (inside \rightarrow outside) that occur as channels shift conformation from the open state to the transition state corresponding to deactivation or inactivation, respectively. Then, from Eq. 2 and elementary Markov theory (15), we can predict that the time constant of open time histograms (T_o) should be related to a biexponential function of V (14):

$$1/T_o = k_d(0) \exp(+Q_d V)/(RT) + k_i(0) \exp(+Q_i V)/(RT) \quad (3)$$

This first prediction of the gating scheme describes well the experimentally observed

D. T. Yue, Department of Biomedical Engineering, The Johns Hopkins University School of Medicine, Baltimore, MD 21205.

J. H. Lawrence and E. Marban, Department of Medicine, The Johns Hopkins University School of Medicine, Baltimore, MD 21205.

*To whom correspondence should be addressed.

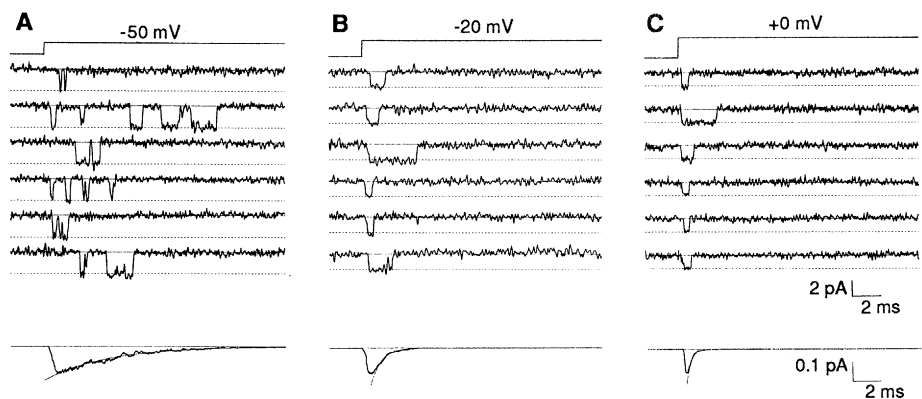


Fig. 1. Different types of gating behavior elicited at various voltages. The representative traces (center) demonstrate multiple reopenings during steps to -50 mV (**A**), but predominantly single openings with steps to -20 mV (**B**), and 0 mV (**C**). The holding potentials were -110 (**A**) and -105 mV (**B** and **C**). The repetition interval was 0.7 s throughout. The ensemble current averages (bottom row) were derived from 400 (**A**) and 361 (**B** and **C**) sweeps. The T_h values were 4.31 (**A**), 0.69 (**B**), and 0.29 (**C**) ms. Records sampled at 100 kHz and filtered at 5 kHz (**A** and **C**) or 2.5 kHz (**B**). All data are from patch R3E73, with four channels.

relation of T_o to V . Because depolarization should promote inactivation and retard deactivation, $Q_i > 0$ and $Q_d < 0$. Thus, Eq. 3 would predict a tendency for T_o to pass through a maximum as voltages are stepped to increasingly positive potentials. Open time histograms obtained from a single patch at different potentials (Fig. 2, **A** to **C**) provide clear-cut support for this prediction, with T_o values of 0.15 , 0.42 , and 0.17 ms corresponding to voltages of -60 , -20 , and $+20$ mV, respectively. In addition, Eq. 3 provides a robust quantitative fit to the relation between reciprocal T_o and voltage, collected from nine patches over a range spanning nearly 100 mV (Fig. 2D). Thus, we estimate equivalent gating charge movements of -1.3 ± 0.2 (Q_d) and $+0.9 \pm 0.2$ (Q_i) electron charges, and zero-potential rate constants of 0.23 ± 0.10 [$k_d(0)$] and 2.6 ± 0.25 [$k_i(0)$] ms^{-1} (18).

The second prediction is that there are two gating patterns, each predominating in the voltage range anticipated from direct inspection of unitary currents (Fig. 1). This prediction follows naturally from the individual exponential components of the fit in Fig. 2D, corresponding to k_d and k_i . At negative potentials (for example, -50 mV), k_d far exceeds k_i , so that every time a channel opens, it very likely returns to C. From C, the channel can return to O, thus giving rise to multiple reopenings, as we observed (Fig. 1A). At a more depolarized potential (such as -20 mV; Fig. 1B), the situation is reversed: k_i predominates over k_d . Here, open channels only infrequently exit to C with the possibility of reopening (Fig. 1B, last trace); open channels are far more likely to exit to I with little chance for reopening (Fig. 1B, other traces). At even more depolarized potentials, there is virtually no chance for deactivation; open channels

leave exclusively to I, so that only single openings are seen (Fig. 1C) (19).

Although the traces in Fig. 1 are in good qualitative agreement with our expectations, we sought to reinforce our interpretation of dual gating patterns (Fig. 3, **A** to **C**) using convolution analysis. Linear systems theory requires that the probability that a channel is open at time t [$p(t)$] be given by the following sum of two convolution integrals (2, 14, 20), which tallies all the ways a channel can be found to be open at time t :

$$p(t) = \int_{x=0}^t f(t-x) L(x) dx + \int_{x=0}^t f(t-x) R(x) dx \quad (4)$$

where $f(t)$ is the probability density that a channel first opens t units of time after the onset of depolarization (first latency density function); $L(x)$ is the probability that a channel will not have closed for x units of time after it opened (lifetime function, equivalent to our open time histograms normalized to unity); and $R(x)$ is the probability that a channel is open x time units after it first opened, given that it closed at least once in the interim (reopening function). The functions L , f , and p (open channel probability) were derived experimentally from a single patch at different potentials (Fig. 3, **A** through **C**). At -50 mV, our scheme predicts frequent O to C transitions (Fig. 3A), with the result that reopenings ought to be plentiful, and R rather large. If this is true, then p should decline substantially more slowly than the convolution of f with L (Eq. 4). The bottom panel of Fig. 3A reveals a large gap between p (upper trace) and the convolution of f with L (lower trace), as predicted at this

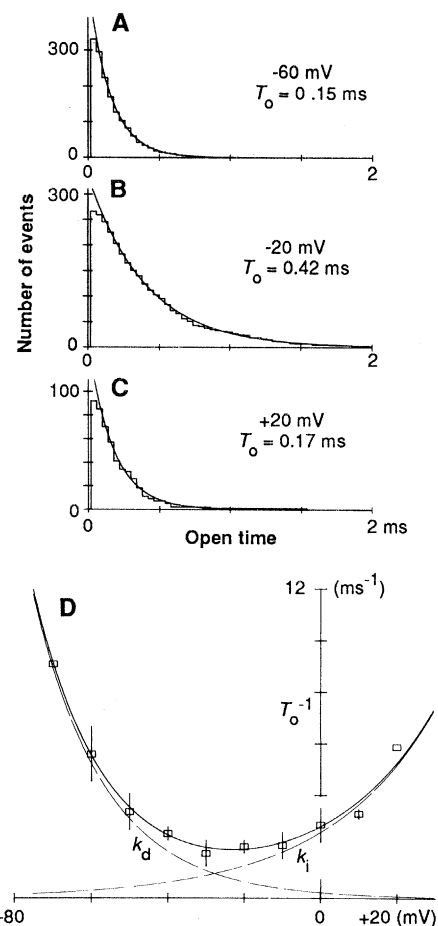


Fig. 2. Interaction of voltage with a single Markov gating model explains the voltage dependence of open times. (**A**, **B**, and **C**) Open time histograms collected from a single patch (R2E76) at -60 (**A**), -20 (**B**), and $+20$ (**C**) mV confirm the prediction that the single-exponential T_o should go through a maximum as voltage is made progressively positive. The bin size was 0.04 ms throughout. (**D**) Quantitative agreement between experimentally determined $1/T_o$ versus V relation and Eq. 3. Thirty-one data points were collected from nine patches. The means, derived from about three patches each, are plotted (\square). SD bars are shown when larger than the symbols. The solid curve is the χ^2 best fit of Eq. 3 to 31 data points. The dashed lines, labeled k_d and k_i , correspond to the individual exponential terms constituting Eq. 3.

voltage. At -20 mV, we anticipate a small but measurable probability for O to C transitions (Fig. 3B). Some reopening would therefore occur, so that R would be small, but not zero. Accordingly, p should exceed the convolution of f with L , but only by a small amount, as the bottom panel of Fig. 3B confirms: here the convolution of f with L falls just below p . If the channel behaves as we envisage at 0 mV (Fig. 3C, top), it cannot reopen; hence, R should be zero. It follows that p should equal the convolution of f with L . In good agreement with our expectation, this convolution faithfully superimposes on p in the bottom panel of Fig. 3C. Another ten patches demonstrated simi-

lar agreement at various voltages between the extent of reopening anticipated from Fig. 2D and that detected by the convolution analysis of large numbers of traces. Such concordance between theory and data, even at extremes of gating behavior and voltage, constitutes an important new feature of this study. The analysis represents strong experimental support for the simple gating subsystem in Eq. 1.

In addition, whereas previous single Na⁺ channel studies have uniformly emphasized marked differences from Hodgkin-Huxley kinetics (16), the convolution analysis reveals remarkable similarities of cardiac channel properties to some features of the classical theory. At voltages positive to -20 mV, our convolution analysis demonstrates that Na⁺ channels open approximately once per depolarization epoch; the sharp *f* traces (Fig. 3, B and C) indicate that channels activate very quickly; and the relatively long *L* traces (Fig. 3, B and C) show that channels inactivate relatively slowly. Because *L* is rate-limiting, *p*, given by the convolution of *f* with *L*, ought to be quite similar to *L* (Fig. 3, B and C). Data from nine patches are pooled in Fig. 3D and demonstrate the crucial physiological consequence of these

Hodgkin-Huxley-like features: at potentials where Na⁺ channels are most active (21), the time constant of decaying ensemble average current (*T_h*) is equivalent to *T_o*. *T_h* was obtained from single-exponential fits of the sort shown in Fig. 1.

The simple interpretation of two sorts of gating in a single type of Na⁺ channel points to an explanation for why some Na⁺ channels generally open once per voltage step (2, 14), whereas others frequently reopen (3-9). The overall character of the voltage dependence of inactivation and deactivation rates in Fig. 2D very likely generalizes to various Na⁺ channel types. Hence, every channel might demonstrate single openings with each step to sufficiently positive potentials where *k_i* predominates, as well as multiple reopenings at sufficiently negative potentials where *k_d* prevails. What would be unique to each Na⁺ channel type are the precise values of *Q_d*, *Q_i*, *k_d*(0), and *k_i*(0); these determine the specific voltage range over which single or multiple channel openings might be observed. Then, depending on the voltage range studied, different Na⁺ channel types would be characterized as predominantly single- or multi-opening in nature. For example, the main difference

between neuroblastoma cells and heart cells arises from the fact that *Q_d* is about twofold larger in neuroblastoma Na⁺ channels [-2.5 to -3.5 electron charges (14)], so that the voltage at which *k_i* would begin to overshadow *k_d* is far more negative (~-50 mV). Hence, the potential range over which single openings would be observed constitutes a much larger portion of the technically accessible voltages. In fact, single openings would be observed at voltages sufficiently negative that activation, rather than inactivation, would be rate-limiting (the converse of the cardiac channel, Fig. 3, B and C).

In contrast to neuronal tissue (14), the equivalent charge movements we determine in cardiac tissue for deactivation (-1.3 electron charges) and inactivation (+0.9 electron charges) are comparable to each other in magnitude. In addition, activation rates at negative potentials such as -50 mV (*p* upstroke in Fig. 3A) are similar to inactivation rates at more positive potentials such as 0 mV (*L* in Fig. 3C). These features raise the interesting possibility that gating charge movements in cardiac muscle may differ from those in neuronal tissue (22) in that there may be observable gating currents associated with both activation and inactivation processes. Such a proposal is now testable with the advent of nonlinear capacity current measurements in heart cells (23).

Our observations show that cardiac Na⁺ channels share in common with those in neuronal cells a simple gating motif, despite marked differences in behavior. We expect that this molecular scheme, although general enough to capture a design theme common to various Na⁺ channels, retains sufficient sophistication to distinguish unique characteristics of each. The overall strategy demonstrated here may therefore prove useful in evaluating the functional consequences of differences in Na⁺ channel structure (24).

Note added in proof. Similar conclusions regarding the relative roles of deactivation and inactivation have been reached (25).

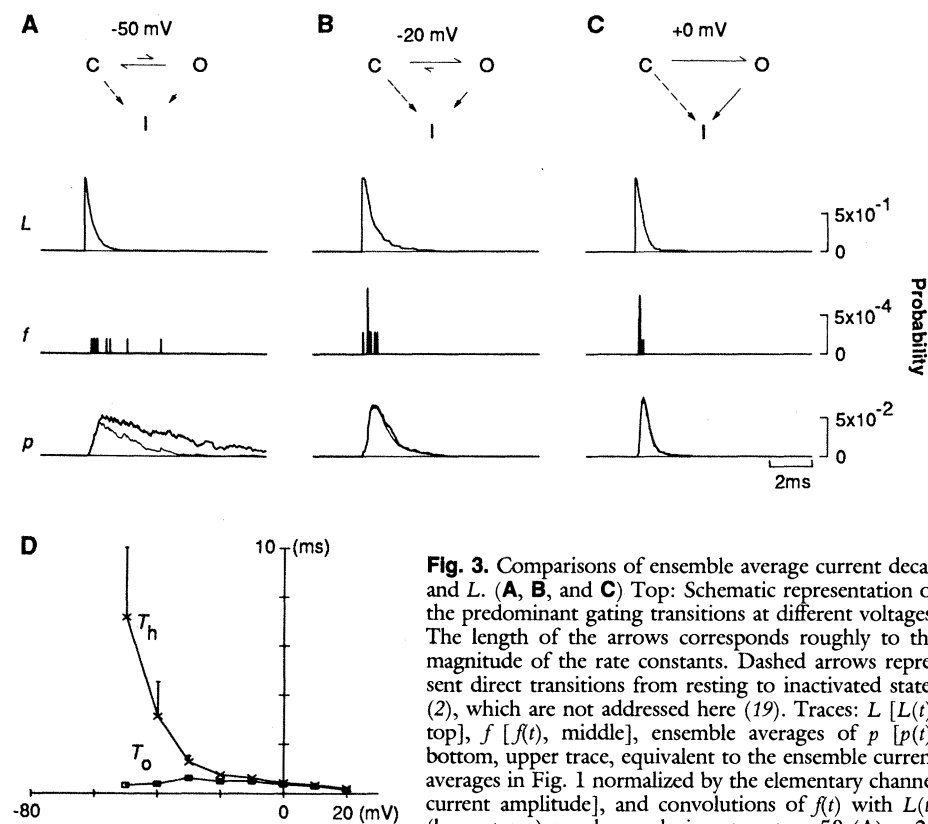


Fig. 3. Comparisons of ensemble average current decay and *L*. (**A**, **B**, and **C**) Top: Schematic representation of the predominant gating transitions at different voltages. The length of the arrows corresponds roughly to the magnitude of the rate constants. Dashed arrows represent direct transitions from resting to inactivated states (2), which are not addressed here (19). Traces: *L* [*L*(*t*), top], *f* [*f*(*t*), middle], ensemble averages of *p* [*p*(*t*), bottom, upper trace, equivalent to the ensemble current averages in Fig. 1 normalized by the elementary channel current amplitude], and convolutions of *f*(*t*) with *L*(*t*) (lower trace) are shown during steps to -50 (A), -20

(B) and 0 (C) mV. These functions correspond to the data in Fig. 1. We calculated *f* from the *n*th root of cumulative *f* values (2) where *n* = 4 was the number of channels in this patch. Convolutions were performed in the discrete-time domain. (D) Voltage dependence of *T_h* (x) and *T_o* (□). *T_h* approaches *T_o* over the voltage range of the plateau of the cardiac action potential. Data were collected from nine patches and the means, derived from about three patches each, are plotted. SDs are shown when larger than the symbols.

REFERENCES AND NOTES

1. M. Noda *et al.*, *Nature* **312**, 121 (1984); L. Salkoff, *Science* **237**, 744 (1987); M. Noda *et al.*, *Nature* **320**, 188 (1986); T. Kayano, M. Noda, V. Flockerzi, H. Takahashi, S. Numa, *FEBS Lett.* **228**, 187 (1988).
2. R. W. Aldrich *et al.*, *Nature* **306**, 436 (1983).
3. C. A. Vandenberg and R. Horn, *J. Gen. Physiol.* **84**, 535 (1984).
4. C. A. Vandenberg and F. Bezanilla, *Biophys. J.* **53**, 226a (1988).
5. A. B. Cachelin, J. E. De Peyer, S. Kokubun, H. Reuter, *J. Physiol. (London)* **340**, 389 (1983).
6. D. L. Kunze, A. E. Lacerda, D. L. Wilson, A. M. Brown, *J. Gen. Physiol.* **86**, 691 (1985).
7. J. B. Patlak and M. Ortiz, *ibid.*, p. 89.
8. A. O. Grant and C. F. Starmer, *Circ. Res.* **60**, 897 (1987); H. A. Fozzard, D. A. Hanck, J. C. Makielski, B. E. Scanley, M. F. Sheets, *Experientia* **43**, 1162 (1987); S. A. Siegelbaum, J. S. Camardo, R. B. Robinson, *Biophys. J.* **49**, 53a (1986).
9. J. B. Patlak and M. Ortiz, *J. Gen. Physiol.* **87**, 305 (1986).

10. B. E. Scanley and H. A. Fozzard, *Biophys. J.* **52**, 489 (1987).
11. Guinea-pig ventricular myocytes were enzymatically dissociated [D. T. Yue and E. Marban, *Pfluegers Arch.* **413**, 127 (1988)]. Pipettes contained 423 mM NaCl, 5 mM Hepes-NaOH, 5 mM KCl, 1 mM MgCl₂, and 5 mM BaCl₂, pH 7.4. The bath contained 37.5 mM KCl, 180 mM potassium glutamate, 15 mM Hepes-KOH, 1.5 mM MgCl₂, 15 mM glucose, and 1 to 2 mM Ca-adenosine triphosphate (ATP), pH 7.3. The high K⁺ in the bath zeroed approximately the membrane potential, enabling estimates of absolute transpatch potentials. Pipettes were fabricated from borosilicate glass (Corning, 7099S-100). Cell-attached recordings, collected \geq 5 min after seal formation, were obtained at 20°C [O. P. Hamill, A. Marty, E. Neher, B. Sakmann, F. J. Sigworth, *Pfluegers Arch.* **391**, 85 (1981)]. An Axopatch 1A amplifier, with a CV-3-1A headstage, was used (Axon Instruments). Signals were lowpass filtered (4-pole Bessel at 5 kHz, -3 dB, unless noted) and digitized (100 kHz, 12-bit resolution) on a PDP-11-73 computer (Indec Systems). Records, corrected for leak and capacity transients by digital subtraction of functions fitted to blank sweeps, were converted to idealized form by half-height criteria [T. A. Hoshi and R. W. Aldrich, *J. Gen. Physiol.* **91**, 73 (1988)] and then used to construct ensemble averages or histograms. Ensemble averages have been normalized for the number of channels in the patch, estimated from the maximum number of overlapping current levels in steps from a hyperpolarized holding potential (\leq -140 mV) (2). Cumulative

open time histograms were fitted with single exponentials by a nonlinear, least-squares minimization procedure, ignoring the first few bins to compensate for missed events (15). Holding potentials were adjusted to produce \geq 60% blank traces, thereby minimizing the occurrence of stacked openings in multichannel patches, and maximizing the likelihood that openings in a given nonblank trace reflected the activity of a single channel ($>$ 80% by binomial analysis). Open time histogram analysis excluded any residual stacked openings. Results from a patch that contained only one channel agreed entirely with those from multichannel patches. Means \pm SD are shown for pooled data. Parameters show 70% confidence intervals (18).

12. B. Nilius, *Biophys. J.* **53**, 857 (1988).

13. P. Hess, J. B. Lansman, R. W. Tsien, *Nature* **311**, 538 (1984).

14. R. W. Aldrich and C. F. Stevens, *J. Neurosci.* **7**, 418 (1987).

15. D. Colquhoun and A. G. Hawkes, in *Single Channel Recordings*, B. Sakmann, E. Neher, Eds. (Plenum, London, 1983), pp. 135-175.

16. A. L. Hodgkin and A. F. Huxley, *J. Physiol. (London)* **117**, 500 (1952).

17. R. W. Aldrich, *Trends Neurosci.* **9**, 82 (1986).

18. N. R. Draper and H. Smith, *Applied Regression Analysis* (Wiley, New York, 1966), pp. 299-301.

19. The exact number of openings at negative voltages (\leq -20 mV) is influenced by C \rightarrow I transitions, quantification of which requires a different analysis (2). Regardless, the primary qualitative prediction by Eq. 1 of reopenings at negative potentials, with

single openings at positive voltages, is insensitive to the precise rate of such transitions. Reopenings require the O \rightarrow C transitions predicted by Eq. 1. Single openings at positive potentials must relate to the O \rightarrow I transitions explained by Eq. 1 because transitions from C \rightarrow O versus C \rightarrow I are increasingly favored at positive voltages (14).

20. D. G. Luenberger, *Introduction to Dynamic Systems: Theory, Models, & Applications* (Wiley, New York, 1979).

21. H. A. Fozzard and M. F. Arnsdorf, in *The Heart and Cardiovascular System: Scientific Foundations*, H. A. Fozzard, R. B. Jennings, E. Haber, H. E. Morgan, Eds. (Raven, New York, 1986), pp. 1-30.

22. F. Bezanilla and C. A. Armstrong, *J. Gen. Physiol.* **70**, 549 (1977).

23. B. P. Bean and E. Rios, *Biophys. J.* **53**, 158a (1988); D. A. Hanck, M. F. Sheets, H. A. Fozzard, *ibid.*, p. 535a.

24. P. M. Vassilev, T. Scheuer, W. A. Catterall, *Science* **241**, 1658 (1988).

25. M. F. Berman, J. F. Camardo, R. B. Robinson, S. A. Siegelbaum, *J. Physiol. (London)*, in press.

26. We thank G. Tomaselli and G. Yellen for their comments on the manuscript. The work was supported by grants from NIH (to E.M., HL36957 and HL01874), from Pfizer (New Faculty, D.T.Y.) and Merck (Fellow, J.H.L.) Pharmaceuticals, and from the American Heart Association, Maryland Affiliate (Young Investigator, D.T.Y.).

24 October 1988; accepted 1 February 1989

Modulation of Rod-Cone Coupling by Light

XIONG-LI YANG* AND SAMUEL M. WU†

Although electrical coupling between rods and cones in the retina has been assumed to be static, it has now been shown that rod-cone coupling can be strengthened by light. Increment threshold measurements reveal that cone input to rods increases progressively as background light becomes brighter. Current injection into cones produces larger responses in adjacent rods in the presence of background light than in darkness. Weak coupling under dark-adapted conditions facilitates synaptic transmission of small rod signals, and strong coupling under light-adapted conditions enhances transmission of large cone signals.

IN THE VERTEBRATE RETINA, RODS AND CONES are electrically coupled to each other by gap junctions (1), and the coupling is thought to be weak and static (2). However, electrical coupling between horizontal cells in the fish and turtle retinas can be modulated by light or by neurotransmitters (3). Moreover, anatomical analysis has indicated that signal transmission from photoreceptors to bipolar cells would be enhanced if the strength of rod-cone coupling varied with light adaptation conditions (4). We therefore studied the effect of steady background light on rod-cone coupling in the tiger salamander retina. We measured (i) increment threshold functions of the rods and cones to 500- and 700-nm light stimuli and (ii) the influence of background light on the voltage responses of rods to current injections into neighboring cones. We also studied the voltage dependence of this light-induced modulation of the rod-cone coupling.

Rods and cones were recorded separately or simultaneously under visual control with infrared illumination in superfused, flat-mounted, isolated retinas from the larval tiger salamander (*Ambystoma tigrinum*) (5). In this retina, there is primarily one type of rod (peak spectral sensitivity around 520 nm) and one type of cone (peak spectral sensitivity around 620 nm) (2, 5). We first studied the effect of background light on the cone and rod responses to 700- and 500-nm test lights (Fig. 1A). The intensities of the two test lights were adjusted so that they evoked responses of the same amplitude in darkness. In the presence of background light, the two cone responses were of similar amplitude, indicating that cones receive little influence from other cells. This does not, however, imply that background light does not affect rod-cone coupling, because rod responses are suppressed when background light is present and thus they cannot influence cones, regardless of any change in

coupling. In contrast to the cone responses, rod responses to the 700- and 500-nm test light in the presence of background light were of different amplitude: the response to 700-nm light was larger than that to 500-nm light. This finding is consistent with the notion that the cone contribution to rod responses is greater in the presence of background light than in darkness.

We then determined the intensity of 500- and 700-nm lights necessary to obtain a 2-mV criterion response as a function of the intensity of a background stimulus (I_B) of 500 nm. This increment threshold data for a cone is shown in Fig. 1B. Under dark-adapted conditions ($I_B = -\infty$), the threshold intensities for both 500- and 700-nm flashes are similar, because the cone pigment in this retina is about equally sensitive to these two wavelengths (5). As I_B increases, the cone response threshold did not change until background light exceeded -5. As I_B increased further, the cone became responsive to the background light, adaptation occurred, and thresholds became elevated. The 500- and 700-nm functions closely correspond to each other throughout the whole range of I_B intensity. This finding indicates that only the cone visual pigment, acting according to the photochemical principle of univariance (6), governed the behav-

Cullen Eye Institute, Baylor College of Medicine, Houston, TX 77030.

*Present address: Shanghai Institute of Physiology, Academia Sinica, Shanghai, China.

†To whom correspondence should be addressed.